Time-Resolved Fluorescence Study of Azurin Variants: Conformational Heterogeneity and Tryptophan Mobility

Sandra J. Kroes,* Gerard W. Canters,* Gianfranco Gilardi,# Arie van Hoek,§ and Antonie J. W. G. Visser§

*Leiden Institute of Chemistry, Gorlaeus Laboratories, 2300 RA Leiden, The Netherlands; #Imperial College of Science, Technology and Medicine, University of London, London SW7 2AZ, England; and §MicroSpectroscopy Centre, Department of Biomolecular Sciences, Laboratory of Biochemistry, Wageningen Agricultural University, 6703 HA Wageningen, The Netherlands

ABSTRACT Time-resolved fluorescence and time resolved fluorescence anisotropy studies have been performed on wild-type azurin from *Pseudomonas aeruginosa* and two variants to study the mobility of Trp^{48}. The two azurin variants in which the microenvironment of Trp^{48} was changed comprised the single mutations $Ile^{7}Ser$ and $Phe^{110}Ser$. The experiments were performed on the holo-Cu(I), holo-Cu(II), and apo- forms at various pH values, viscosities, and temperatures; two distinct parts of the emission spectrum were selected for detection. Two prominent subnanosecond lifetimes in the fluorescence decays of the Cu(II) proteins could be observed. The decay of apo-azurin also consists of more than one component. The occurrence of more than one component in the fluorescence decays is explained by conformational heterogeneity. The anisotropy decay results appeared to be different for wild-type and mutated azurins. $Phe^{110}Ser$ and $Ile^{7}Ser$ azurin show more mobility of the Trp^{48} residue, as reflected in the order parameter.

INTRODUCTION

With the advent of site-directed mutagenesis it has become possible to probe the stability and dynamics of a protein by making point mutations in its primary sequence. Studies of this type can be of crucial importance for the identification of the determinants of the fold of a particular protein and for providing insight into how side-chain packing is connected with the fluxionality of the protein interior. Proteins with a large stability in the native state are ideal for this kind of study, because it may be expected that they can tolerate a local disturbance of their three-dimensional framework without undergoing a major disruption or unfolding of their overall structure. Thus the local effects of the point mutation can be scrutinized. Two main techniques have gained popularity for the study of internal protein dynamics: time-resolved fluorescence and heteronuclear multidimensional NMR on ^{15}N-enriched proteins. The present study focuses on azurin from *Pseudomonas aeruginosa*, which is an example of such a robust protein. We report the effect of two point mutations on the mobility of Trp^{48} as studied by various fluorescent spectroscopy techniques.

Azurin functions as an electron carrier in a variety of denitrifying bacteria. It is a member of the class of the small blue copper proteins whose unique spectroscopic properties have made them the object of many experimental and theoretical studies. Oxidized blue copper proteins display an intense optical absorption around 600 nm and an unusually small hyperfine splitting in the electron paramagnetic resonance (EPR) spectrum (35×10^{-4} $cm^{-1} < A_{\|} < 70 \times 10^{-4}$ cm^{-1}; Solomon et al., 1992). The x-ray structure of azurin from *P. aeruginosa* is known (Adman and Jensen 1981; Nar et al., 1991b). The protein consists of one α-helix and eight β-strands that form two β-sheets in a Greek-key folding motif (Adman, 1991). The β-sandwich is closely packed and forms a highly hydrophobic core. *P. aeruginosa* azurin has only one tryptophan residue, Trp^{48}, pointing with its side chain to the center of the hydrophobic core of the protein (Fig. 1).

When excited with ultraviolet light, apo-azurins from different bacterial sources exhibit a strong fluorescence, which has been attributed to their tryptophan residues. With a few exceptions, buried tryptophan residues in proteins show emission maxima in the lower energy range of 325–335 nm (Burstein et al., 1973), but upon excitation of azurin at 280–300 nm, a structured fluorescence is seen with a maximum at 306–308 nm (Finazzi-Agrò et al., 1970). While the fluorescence spectrum of holo-azurin is similar to that of the apo-protein, the emission is strongly quenched by the presence of the copper. The precise mechanism of the quenching is still under debate (Petrich et al., 1987; Sweeney et al., 1991; Hansen et al., 1990). A special role has been assigned to Trp^{48} within the context of long-range electron transfer studies. Experimental results obtained on azurin in which the S-S bridge (Cys^{3}-Cys^{26}) had been reduced to $RSSR^{-}$ by CO_2^{-} radical anions, appeared compatible with two electron transfer pathways from $RSSR^{-}$ to Cu(II). Trp^{48} is involved in one of them. The electron coupling pathway runs from the indole ring of Trp^{48} via Val^{49} and Phe^{111} (H-bond) to the copper ligand Cys^{112} (Farver et al., 1996).

For many years it has been thought that the fluorescence decay of apo-azurins exhibits a single exponential behavior, whereas the decay of holo-azurins contains more than one component (Grinvald et al., 1975; Munro et al., 1979; Szabo et al., 1983). Hutnik and Szabo distinguished three compo-

Received for publication 24 July 1997 and in final form 27 July 1998.

Address reprint requests to Dr. G. W. Canters, Leiden Institute of Chemistry, Gorlaeus Laboratories, Leiden University, P.O. Box 9502, 2300 RA Leiden, The Netherlands. Tel.: 31-71-5274256; Fax: 31-71-5274349; E-mail: canters@chem.leidenuniv.nl.

0006-3495/98/11/2441/10 $2.00

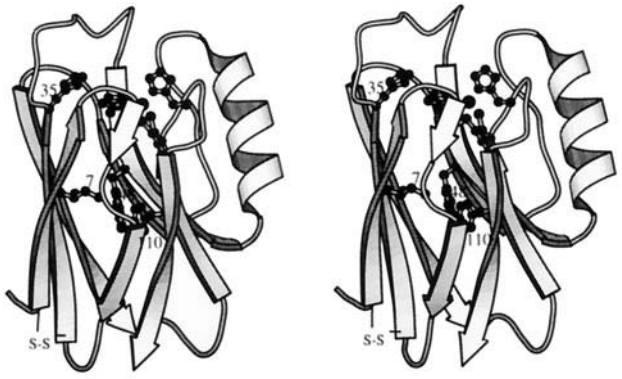

FIGURE 1 MOLSCRIPT plot (Kraulis, 1991) of wild-type azurin from *P. aeruginosa* (Nar et al., 1991b). The side chains of Trp^{48}, Phe^{110}, His^{35}, and Ile^{7} are indicated, as are the side chains of the Cu ligands (His^{46}, His^{117}, Cys^{112}, and Met^{121}).

nents for the holo-azurin fluorescence decay (Hutnik and Szabo, 1989a,b). They also concluded that the multiexponential decay of holo-azurin originates from conformational heterogeneity and not from contamination by an apo-form (Petrich et al., 1987).

To get more insight into the dynamical properties of Trp^{48} in azurin, we constructed two azurin mutants: $Ile^{7}Ser$ and $Phe^{110}Ser$. Both Ile^{7} and Phe^{110} are close to Trp^{48}, so their mutation may be expected to affect the environment of this Trp (Fig. 1). The Ser side chain in both cases occupies a smaller volume than the native residue and introduces a larger polarity in the hydrophobic core. The aim is to see how changes in the microenvironment of Trp^{48} affect the dynamics of this Trp.

Steady-state fluorescence experiments, particularly on the apo-forms of these mutants (Gilardi et al., 1994; Mei et al., 1996), have shown that the emission maximum of the Trp fluorescence may exhibit a red-shift, depending on the excitation wavelength. Time-resolved fluorescence spectroscopy also revealed changes in the fluorescence lifetimes and in the distribution of the lifetimes of the mutants; these variations were interpreted in terms of a change in solvation of the Trp^{48} side chain.

In the present work we have performed a detailed study of the time-resolved fluorescence and fluorescence anisotropy to see how the mobility of Trp^{48} is influenced by the two mutations. The fluorescence and fluorescence anisotropy decays were measured for the Cu(I), the Cu(II), and the apo-forms of wild-type (wt), $Phe^{110}Ser$ and $Ile^{7}Ser$ azurins. As a protein in solution constitutes a large ensemble of molecules with different conformations, we used red-edge excitation (300 nm) to select a subensemble with a minimal conformational heterogeneity (Bastiaens et al., 1992). In addition, by using red-edge excitation, the fundamental anisotropy of Trp is distinctly higher (Demchenko, 1992). The experiments were done at different pH values, viscosities, and temperatures, and the detection wavelength was set at two values: in the center at 321 nm and in the red part at 349 nm of the emission spectrum.

EXPERIMENTAL

Sample preparation

The procedure of the isolation and purification of wt *P. aeruginosa* azurin has been described by van de Kamp et al. (1990). Details about the site-directed mutagenesis procedure, the protein expression, the isolation, and the purification of the $Ile^{7}Ser$ and $Phe^{110}Ser$ mutants have been described elsewhere (Gilardi et al., 1994).

All fluorescence measurements were performed in 20 mM HEPES buffer at pH 7.5 or in 50 mM phosphate buffer at pH 5.5. The protein absorbance was around 0.05 at the excitation wavelength. The purity of oxidized protein was verified with isoelectric focusing (IEF) electrophoresis and ultraviolet-visible (UV-Vis) spectroscopy. The A_{628}/A_{280} ratio was 0.60 for the samples used in this study (Gilardi et al., 1994).

The reduction of Cu(II) azurin was performed by adding aliquots of a solution of 0.1 M sodium dithionite in 0.1 M NaOH. We added a 10 times molar excess of sodium dithionite with respect to the protein in the fluorescence cuvette and measured the fluorescence directly after the protein became colorless. In the cuvette with the blank, the same sodium dithionite concentration was present. To study the effect of viscosity, the samples were brought to 40% (v/v) glycerol by gently mixing 600 μl from the sample with 400 μl of 100% glycerol (fluorescence microscopy grade; Merck, Darmstadt, Germany). Care was taken that the protein had the same concentration as in the samples without glycerol. The apo-proteins were prepared from holo-azurins by adding potassium cyanide and EDTA to final concentrations of 0.1 M potassium cyanide and 1 mM EDTA in 0.15 M 2-amino-2-hydroxymethylpropane-1,3-diol-HCl (Tris-HCl) (pH 8), followed by column chromatography (van de Kamp et al., 1990).

Time-resolved fluorescence and fluorescence anisotropy measurements

The polarized time-resolved fluorescence decay curves of azurin were acquired using excitation with 4-ps laser pulses and detection with the time-correlated single photon counting technique, as described in detail elsewhere (Pap et al., 1993; Visser et al., 1994). The wavelength of excitation was 300 nm; the wavelength of detection was selected, depending on the experimental requirements, by using different interference filters (λ_{maxT} = 321.4 nm, bandwidth 6.3 nm, full width at half-maximum, FWHM, or λ_{maxT} = 348.8 nm, bandwidth 5.4 nm FWHM; Schott, Mainz, Germany), in combination with a WG 320 cutoff filter (Schott). For deconvolution of the experimental data, the dynamic instrumental response of the setup was recovered using the fast, single-exponential decay of *p*-terphenyl (25 ps) in a mixture of cyclohexane and CCl_4 in a 3:1 volume ratio (Visser et al., 1994). The instrumental response function (see Fig. 2) has a FWHM of ~60 ps. The experiments were performed with the samples in quartz cuvettes (1-cm pathlength) placed in a thermostatted holder (20, 27, 34, and 40°C). The data were collected in a multichannel analyzer, using 1024 channels with a channel spacing of 16.5 ps.

Data analysis

Experimental data were transferred to a Silicon Graphics workstation for data analysis. Analysis of the (multiexponential) decay of the fluorescence intensity and of the fluorescence anisotropy was performed by using two different techniques: the maximum entropy method (MEM) (Maximum Entropy Solutions, Ely, England) described by Livesey and Brochon (1987) and Brochon (1994) and the global analysis (GA) method (software obtained from Globals Unlimited, Urbana, IL) described by Beechem et al. (1992). The principles and applications of those two programs have been described in the literature (Bastiaens et al., 1992; Leenders et al., 1993; Kim et al., 1993). The MEM method is more versatile in the sense that it produces a continuous lifetime distribution function, whereas the GA method only provides single lifetimes, in other words, the "distribution function" in this case consists of "sticks" of different amplitudes on the lifetime axis. The amplitudes belonging to the distributed lifetimes ob-

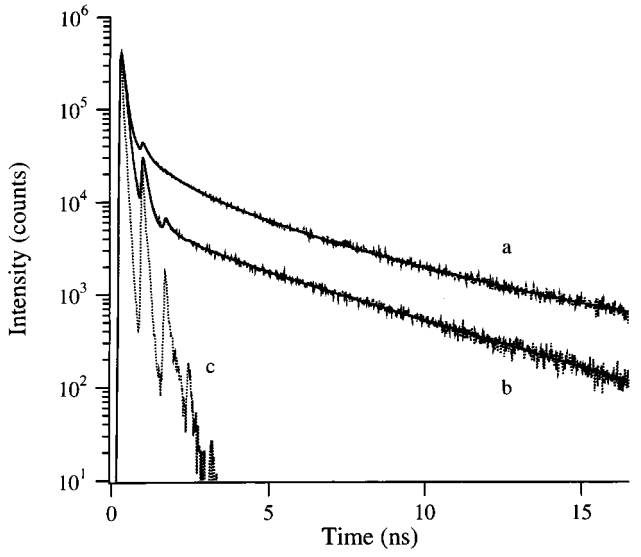

FIGURE 2 (*a* and *b*). Experimental (·····) and fitted (——) fluorescence decay curves of *P. aeruginosa* wt Cu(II)-azurin at pH 7.5, 20°C, and two detection wavelengths, 349 nm (*a*) and 321 nm (*b*). (*c*) Experimental response function obtained at λ_{det} = 321 nm from a quenched *p*-terphenyl solution in a mixture of cyclohexane and CCl_4 (3:1 volume ratio). For clarity, curves *a* and *c* are normalized to the maximum of curve *b*. The peaks in curve *c* are caused by reflections at the lens, the filter, and the photocathode surface. The fitted curves *a* and *b* are reconvoluted with the instrumental response function and illustrate that these instrumental artefacts can be accounted for in the analysis.

tained with the MEM method are integrated peak areas, and their values are similar to the corresponding "stick" values obtained by the GA method.

Using the GA method, the total fluorescence decay of Trp in azurin is modeled as a sum of exponentials,

$$I(t) = \sum_{i=1}^{n} (\alpha_i e^{-t/\tau_i}) \quad (1)$$

in which α_i is the preexponential factor belonging to the lifetime component τ_i and n is the minimum number of lifetimes needed to obtain an acceptable fit to the data. For holo-azurin fluorescence decays n was 4 or 5, whereas for apo-azurin decays this value was 3. The error in the calculated fluorescence (χ^2) is minimized and calculated according to

$$\chi^2 = 1/M \sum_{k=1}^{M} [(I_k^{calc} - I_k^{obs})/\sigma_k]^2 \quad (2)$$

where the superscripts calc and obs on I denote the calculated and observed intensity in channel k of the multichannel analyzer. M is the total amount of channels used in the analysis of the fluorescence decay, and σ_k is the standard deviation in channel k.

The experimental observable in a time-resolved fluorescence anisotropy experiment is the fluorescence anisotropy, defined as (Lakowicz, 1983)

$$r(t) = \{I_\parallel(t) - I_\perp(t)\}/\{I_\parallel(t) + 2I_\perp(t)\} \quad (3)$$

where $I_\parallel(t)$ and $I_\perp(t)$ are the observed time-dependent components of the fluorescence that are polarized parallel and perpendicular relative to the polarization direction of the exciting beam, respectively. In the data analysis $I_\parallel$ and $I_\perp$ are simultaneously fitted by the global analysis approach according to the model of Eq. 4 (see below). The fluorescence anisotropy experiments in principle probe two processes: first, the rapid internal motion of the probe within the protein (characteristic time: ϕ_{int}) and second, the protein rotational motion as a whole (characteristic time: ϕ_{prot}). The anisotropy (Eq. 3) can be modeled using the following expression (Dorovska-Taran et al., 1993):

$$r(t) = \{\beta_1 \exp(-t/\phi_{int}) + \beta_2\}\exp(-t/\phi_{prot}) \quad (4)$$

β_1 and β_2 are the preexponential amplitudes of these rotational motions. In the GA method we assume that all fluorescence components contribute in a similar way to the anisotropy, although the shorter lifetimes (<0.1 ns) will not have any influence at longer times (>2 ns). This is the so-called nonassociative case. In the data analysis $I_\parallel(t)$ and $I_\perp(t)$ are simultaneously fitted in a global analysis according to the model of Eq. 4 (details of the fitting procedure are presented by Bastiaens et al., 1992). From β_1 and β_2 the order parameter S can be calculated from (Dorovska-Taran et al., 1993)

$$S^2 = \beta_2/(\beta_1 + \beta_2) \quad (5)$$

When $S^2 = 0$ the internal motion of Trp is completely isotropic; if $S^2 = 1$ the residue is fixed in the molecular frame and only protein rotation is observed. Generally, the anisotropy decay data were fitted with one (β_1 = 0 in Eq. 4) and two (β_1 and $\beta_2 = 0$ in Eq. 4) correlation times. When the quality criterion of the fit (Eq. 2) did not significantly improve with two correlation times, it was assumed that a single-component anisotropy decay adequately described the data.

In the so-called wobbling-in-cone model (Kinosita et al., 1977), where the internal motion corresponds to free diffusion in a cone with semiangle θ, the order parameter is related to θ according to (Lipari and Szabo, 1982)

$$S^2 = [1/2 \cos\theta(\cos\theta + 1)]^2 \quad (6)$$

From Eq. 6, the value of the angle θ can be estimated from the experimentally determined value of S. From the correlation time of restricted motion (ϕ_{int}) one obtains the diffusion coefficient for the restricted internal motion $D_\perp$ from (Szabo, 1984)

$$D_\perp = (1 - S^2)/(6\phi_{int}) \quad (7)$$

RESULTS

The total fluorescence decay and fluorescence anisotropy of holo- and apo-wt, $Phe^{110}Ser$ and $Ile^{7}Ser$ azurin were studied under a variety of conditions. Red-edge excitation (300 nm) was used to photoselect a subpopulation of protein molecules from the total ensemble of protein conformers and to maximize the emission polarization anisotropy (Demchenko, 1992; Lakowicz and Keating-Nakamoto, 1984). Two wavelengths representing "central" and "red" emission (321 nm and 349 nm, respectively) were selected for the detection. Furthermore, the pH, the temperature, and the viscosity were varied. MEM was used to analyze the time dependence of the total fluorescence data. Application of the GA method did not give significantly different results. MEM failed to give consistent results in the analysis of the fluorescence anisotropy data, and for that case the GA method was used.

Total fluorescence decay

Examples of typical experimental and MEM-fitted fluorescence decays are given in Fig. 2, in which the detection wavelength was set at 349 nm (Fig. 2 *a*) and 321 nm (Fig. 2 *b*), respectively. The lifetime distributions for Cu(II)- and

apo-azurin are shown (wt and both mutants) under a variety of conditions in Fig. 3, *A–D*. The small peak around 0.01–0.02 ns in the lifetime distribution of some of the apo-proteins is an artefact related to the fluorescence properties of the reference compound. It is possible to see the effect of changing the detection wavelength in going from Fig. 3 *A* to Fig. 3 *B*, the effect of lowering the pH from 7.5 to 5.5 in going from Fig. 3 *B* to Fig. 3 *C*, and the effect of changing the viscosity in going from Fig. 3 *C* to Fig. 3 *D*, on the lifetime distributions. The apo-azurin fluorescence decays have a dominant lifetime around 4.5–5.0 ns (Fig. 3 and Table 1), in contrast with holo-azurin, which shows two main lifetimes below 0.2 ns. In the latter case a third small peak between 0.2 and 1 ns is often present, but only when $\lambda_{det} = 349$ nm (less than 3% contribution). Finally, two small peaks contributing less than 2% are found around 1.3 and 4.2 ns for holo-azurin.

An example of the experimental fluorescence decay of the reduced Cu(I) form of wt azurin and the MEM-fitted decay is given in Fig. 4 *A*. The lifetime distributions, recovered by the MEM program, of wt azurin and the two azurin variants, are presented in Fig. 4 *B*. The data are summarized in Table 1, in which the amplitudes and lifetimes of the two main components in the fluorescence decay of the holo-azurins are given. For the apo-proteins the three main components are given.

Fluorescence anisotropy decay

An example of an anisotropy decay is given in Fig. 5, which shows the decays of holo (Fig. 5 *a*) and apo (Fig. 5 *b*) Ile^{7}Ser azurin at $\lambda_{det} = 349$ nm. The results obtained with the GA method are given in Table 2. The anisotropy data were fitted with one ($\beta_1 = 0$) and two (β_1 and $\beta_2 \neq 0$ in Eq. 4) correlation times. When the quality criterion of the fit (Eq. 2) did not significantly improve with two correlation times, the single component description was chosen. The latter case was often obtained for the experiments in which the detection wavelength was set at 321 nm, whereas with the detection wavelength set at 349 nm, two components were nearly always observed that corresponded to overall rotation (ϕ_{prot}) and internal motion (ϕ_{int}). The data are gathered in Table 2. The initial anisotropy $r(0)$, which is almost two times higher for the mutants than for wt azurin, is also given.

DISCUSSION

Total fluorescence decay

The fluorescence decay of apo-azurin consists of one main component around 4.5–5.0 ns and two shorter components with a smaller amplitude (Fig. 3). By contrast, the fluorescence decay of Cu(II)-azurin consists of two main components with short lifetimes (Table 1) and two or three longer-lived components. The small size of the latter (not more than a few percent of the overall lifetime distribution) precludes a firm conclusion about their origin. It should be realized that the large dynamic range of detection (five to six decades of intensity) in the present experimental set-up allows the observation of minute amounts of impurities as opposed to the previously used phase fluorimetry technique (dynamic range: two to three orders of magnitude) (Gilardi et al., 1994; Mei et al., 1996). It was checked whether the small peaks in the Cu(II)-azurin lifetime distribution function might derive from small contaminations, by fitting the fluorescence decay of the Cu(II)-azurin with Eq. 1 and $n = 5$, and fixing three of the five lifetimes at the apo-protein values. A good fit of the data was obtained. Thus a contamination with apo-azurin cannot be excluded on the basis of the experimental findings. Similarly, contamination with a minute amount of Zn(II) azurin, which has a main lifetime of ~4.9 ns (van de Kamp et al., 1990), cannot be ruled out. At the same time, we note that the small 0.2–1 ns component observed for holo-azurin under 349 nm detection is absent from the lifetime distribution function of apo-azurin. Furthermore, the amplitude ratios of the two long-lived components are different for holo- and apo-azurin, and, so, the long-lived components in the Cu(II)-azurin decay cannot be due solely to an apo-contamination. In view of these uncertainties, we refrain from further speculation about the origin of the (small) long-lived components in the lifetime distribution of Cu(II)-azurin and concentrate on the two main (short) components of the fluorescence decay of the holo-protein fluorescence and the three components we observed for the decay of the apo-protein fluorescence.

We ascribe the occurrence of more than one component to conformational heterogeneity in the environment of Trp^{48}. The multicomponent nature of the azurin emission has been observed before, and various causes for it have been proposed in the literature. Szabo and co-workers (Szabo et al., 1983; Hutnik and Szabo, 1989a) have stated that heterogeneity of the fluorescence decay may be connected to different conformations of the Cu and its immediate environment (tetrahedral versus trigonal), although the spectroscopic fingerprint for two conformations of the Cu site (Canters and Gilardi, 1993) is not evident in the optical spectra. Alternatively, conformational heterogeneity may be caused by residue Ile^7, which occurs in two alternative conformations in the x-ray structure, namely, with its side chain eclipsed or staggered with respect to the main chain (Nar et al., 1991a,b). Different structural rigidities in the vicinity of the Trp residue were also invoked by Hansen et al. (1996), who performed time-resolved phosphorescence experiments on wt azurin to explain the occurrence of different decay components.

Ile^7 is partly in van der Waals contact with Trp^{48}. In view of the general sensitivity of the fluorescence lifetime of a Trp residue to its immediate environment, the microheterogeneity of Ile^7 may be considered a plausible source for the observed heterogeneity of the Trp lifetime in the wt Cu(II)-azurin (Nar et al., 1991a,b). In line with this is the observation of pronounced effects of the Ile^{7}Ser mutation on the lifetime distribution when 349-nm detection is used. How-

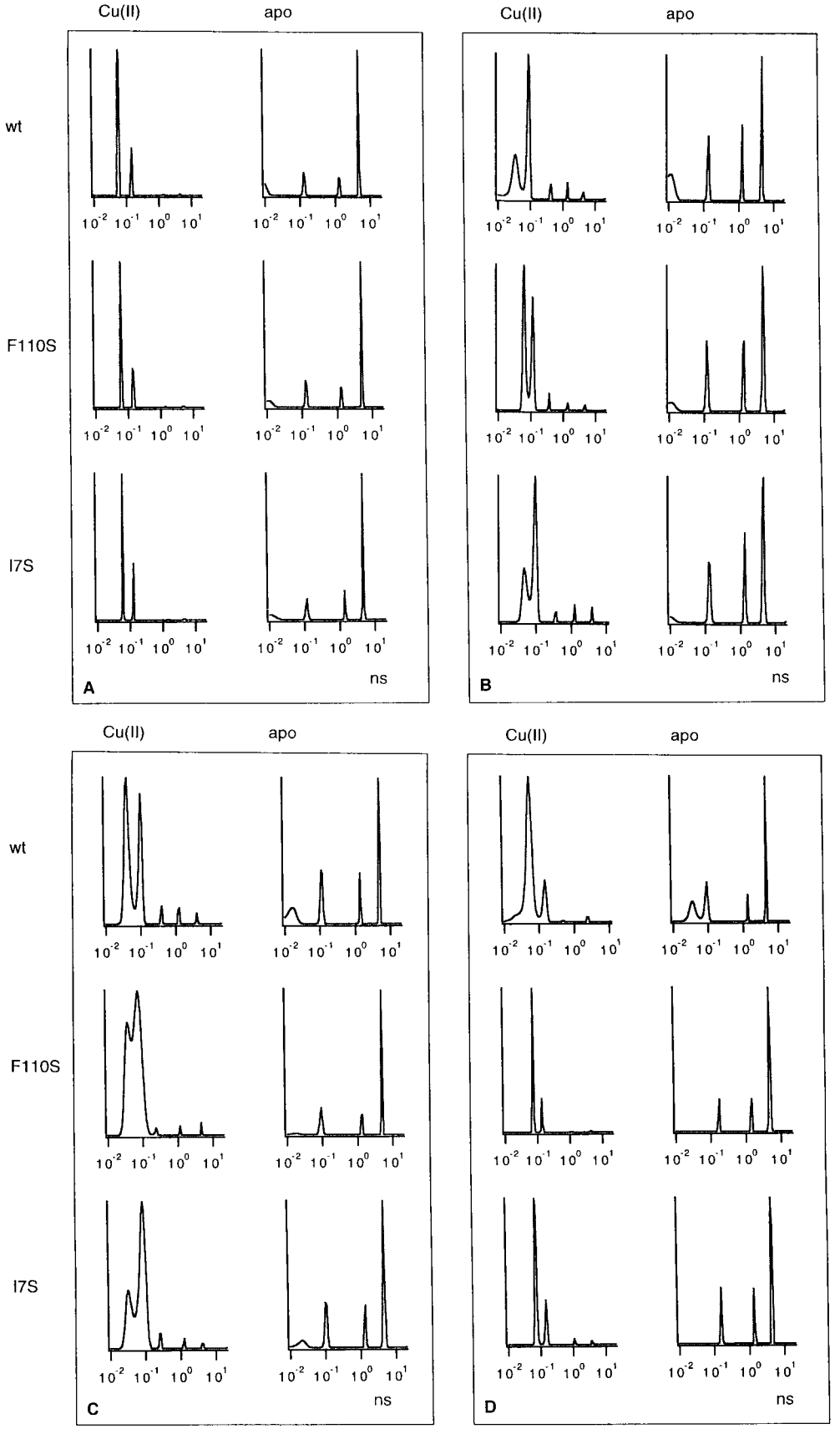

FIGURE 3 Distributions of lifetimes (*normalized linear vertical scale*) for apo and oxidized holo *P. aeruginosa* wt, Phe^{110}Ser and Ile^{7}Ser azurin, calculated by MEM analysis. Horizontal (logarithmic) scale: τ in ns. The experiments were performed at 20°C. (*A*) λ_{det} = 321 nm, pH 7.5. (*B*) λ_{det} = 349 nm, pH 7.5. (*C*) λ_{det} = 349 nm, pH 5.5. (*D*) λ_{det} = 349 nm, pH 5.5, 40% glycerol.

TABLE 1 Total fluorescence decay parameters at 20°C as extracted from the experimental decays by means of the MEM routine

Protein	λ_{em} (nm)	$\alpha 1$	$\tau 1$ (ns)	$\alpha 2$	$\tau 2$ (ns)	$\alpha 3$	$\tau 3$ (ns)	χ^2
Oxidized, pH 7.5								
wt	321	0.80 (0.01)	**0.06** (0.01)	0.20 (0.01)	0.14 (0.01)			2.4
	349	0.39 (0.12)	0.03 (0.01)	0.53 (0.10)	**0.09** (0.01)			1.1
I7S	321	0.71 (0.02)	**0.06** (0.01)	0.28 (0.02)	0.13 (0.01)			1.7
	349	0.35 (0.14)	0.05 (0.01)	0.59 (0.14)	**0.10** (0.01)			1.1
F110S	321	0.72 (0.01)	**0.06** (0.01)	0.27 (0.01)	0.14 (0.01)			1.8
	349	0.57 (0.11)	**0.06** (0.01)	0.39 (0.11)	0.12 (0.01)			1.0
Oxidized, pH 5.5								
wt	321	0.79 (0.01)	**0.05** (0.01)	0.20 (0.01)	0.14 (0.01)			2.1
	349	0.59 (0.10)	**0.04** (0.01)	0.36 (0.10)	0.10 (0.01)			1.1
I7S	321	0.70 (0.01)	**0.05** (0.01)	0.29 (0.01)	0.12 (0.01)			1.8
	349	0.28 (0.12)	0.03 (0.01)	0.68 (0.13)	**0.08** (0.01)			1.0
F110S	321	0.78 (0.01)	**0.05** (0.01)	0.21 (0.01)	0.12 (0.01)			1.8
	349	0.39 (0.17)	0.04 (0.01)	0.58 (0.18)	**0.08** (0.01)			1.1
Reduced, pH 5.5								
wt	349	0.73 (0.05)	**0.03** (0.01)	0.19 (0.04)	0.08 (0.01)			1.1
I7S	349	0.48 (0.02)	**0.06** (0.01)	0.51 (0.01)	**0.16** (0.01)			1.3
F110S	349	0.42 (0.02)	**0.05** (0.01)	0.56 (0.01)	**0.14** (0.01)			2.9
Apo, pH 7.5								
wt	321	0.16 (0.02)	0.13 (0.01)	0.12 (0.01)	1.31 (0.05)	0.61 (0.05)	**4.71** (0.01)	1.3
	349	0.21 (0.02)	0.13 (0.01)	0.16 (0.02)	1.25 (0.04)	0.36 (0.03)	**4.58** (0.04)	1.3
I7S	321	0.16 (0.02)	0.11 (0.01)	0.13 (0.01)	1.38 (0.06)	0.61 (0.05)	**4.65** (0.02)	1.3
	349	0.24 (0.02)	0.13 (0.01)	0.23 (0.02)	1.34 (0.04)	0.49 (0.03)	**4.50** (0.05)	1.2
F110S	321	0.19 (0.02)	0.13 (0.01)	0.13 (0.01)	1.31 (0.05)	0.56 (0.04)	**5.04** (0.01)	1.4
	349	0.23 (0.02)	0.12 (0.01)	0.22 (0.02)	1.32 (0.04)	0.47 (0.03)	**4.80** (0.05)	1.2
Apo, pH 5.5								
wt	321	0.27 (0.02)	0.10 (0.01)	0.12 (0.01)	1.26 (0.03)	0.61 (0.01)	**4.86** (0.01)	1.2
	349	0.25 (0.04)	0.11 (0.01)	0.12 (0.02)	1.38 (0.05)	0.39 (0.05)	**4.90** (0.02)	1.2
I7S	321	0.22 (0.04)	0.10 (0.01)	0.13 (0.01)	1.33 (0.04)	0.52 (0.05)	**4.66** (0.01)	1.3
	349	0.23 (0.04)	0.10 (0.01)	0.14 (0.01)	1.33 (0.06)	0.51 (0.04)	**4.62** (0.03)	1.3
F110S	321	0.20 (0.03)	0.12 (0.01)	0.12 (0.01)	1.36 (0.05)	0.49 (0.05)	**5.00** (0.02)	1.3
	349	0.26 (0.04)	0.09 (0.01)	0.14 (0.01)	1.31 (0.04)	0.57 (0.05)	**4.99** (0.01)	1.3

Standard errors are given in parentheses. A value of 0.01 means that the error is ≤0.01. Main lifetimes are given in bold.

ever, at the same time the relatively small effect of this mutation under 321-nm detection is puzzling in this respect. This is a subject of further study.

The interconversion of the different conformations is not very fast on the time scale of the fluorescence lifetime; otherwise a lifetime distribution with a single peak would have been obtained. When using a simple Arrhenius expression for the rate of transition between two conformations, k_t,

$$k_t = k_a e^{-E_a/RT} \tag{8}$$

one finds with $k_a = 10^{13}\ s^{-1}$ and using an upper limit of $0.1 \times 10^9\ s^{-1}$ for k_t, that the lower limit of the activation energy amounts to $E_a \geq 17.1$ kJ/mol. (R is the gas constant, and T is the absolute temperature.)

The effect of varying several experimental parameters on the fluorescence characteristics have been shown in Fig. 3, and the data have been collected in Table 1. The effect of a temperature increase from room temperature up to 40°C on the spectra of apo- and holo-azurin is minor (data not shown), and no striking effects were observed, except for a minor shortening of the lifetimes (5–10%).

The effect of changing the detection wavelength from 321 nm to 349 nm is larger and unexpected (compare Fig. 3 *A* with Fig. 3 *B*). For apo-azurin the amplitudes of the short-lived components increase. For holo-azurin the amplitude of the longer lifetime component increases dramatically, and the lifetime distributions become broader, indicating increased microheterogeneity around the Trp at red-edge detection. A possible reason why a similar broadening is absent in the apo- forms is that there is sufficient flexibility in the apo-proteins for the microheterogeneity to be averaged out on the time scale of the fluorescence decay.

There is also an effect observed when the pH is lowered from 7.5 to 5.5 (compare Fig. 3 *B* with Fig. 3 *C*). For apo-azurin we see a significantly higher amplitude of the long-lived component, whereas for holo-azurin again some additional broadening can be seen for the two main components. Furthermore, the ratio of the amplitudes of these

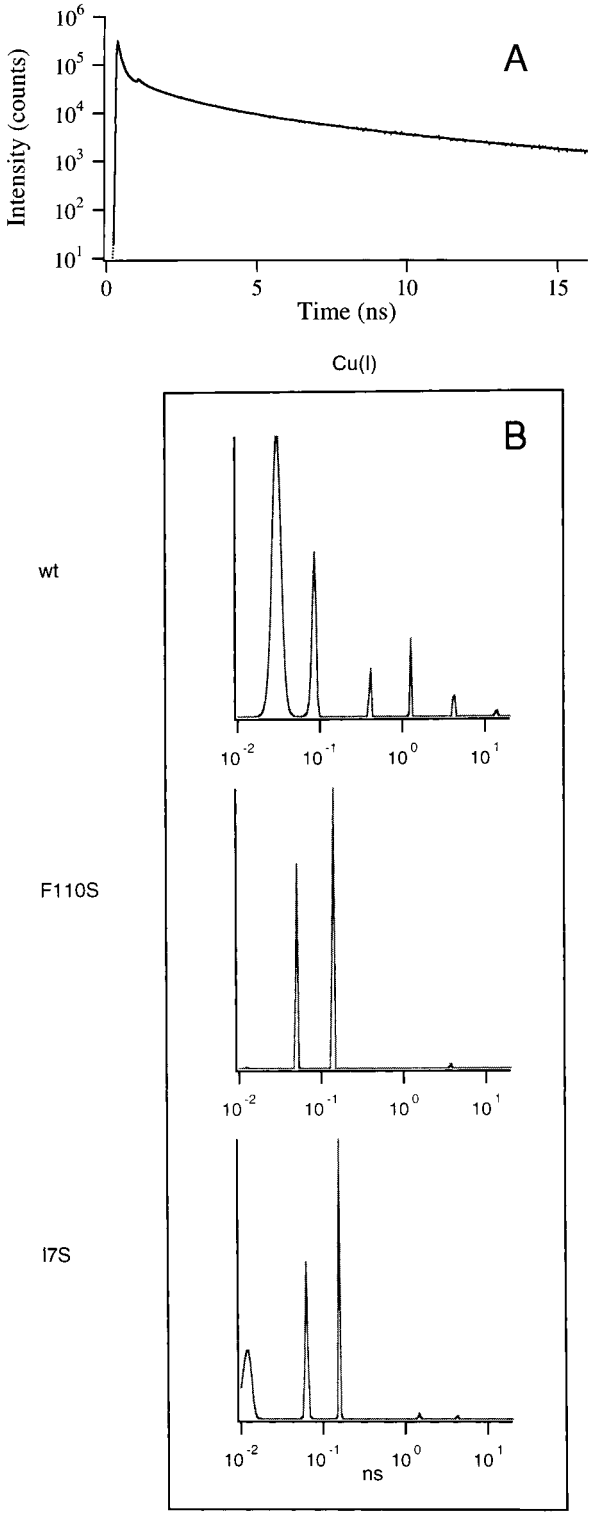

FIGURE 4 (*A*) Experimental (·····) and fitted (——) fluorescence decay curves of reduced *P. aeruginosa* wt Cu(I)-azurin at pH 5.5, 20°C, and λ_{det} = 349 nm. At the scale of the figure the fitted curve cannot be distinguished against the background of the experimental noise. (*B*) Distributions of lifetimes (*normalized linear vertical scale*) for reduced Cu(I)-*P. aeruginosa* wt, Phe^{110}Ser and Ile^{7}Ser azurin (*from top to bottom*) calculated with MEM analysis. The experiments were performed at 20°C, pH 5.5, and λ_{det} = 349 nm. Horizontal (logarithmic) scale: τ in ns.

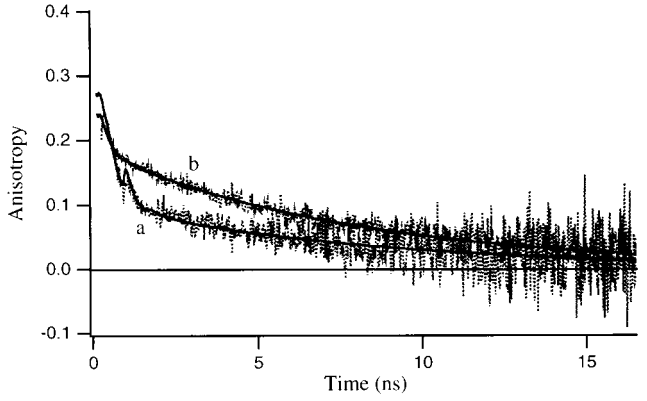

FIGURE 5 Anisotropy decay curves of *P. aeruginosa* Ile^{7}Ser azurin at pH 7.5, 20°C, with the detection wavelength set at 349 nm. (*a*) Experimental and fitted decay of Cu(II) Ile^{7}Ser azurin and (*b*) experimental and fitted decay of apo Ile^{7}Ser azurin.

two components is changed (Table 1). It is known that residue His^{35} in *P. aeruginosa* azurin is involved in a slow exchange between its protonated and nonprotonated forms with a $pK_a \approx 6$ for the oxidized form and 7.2 for the reduced form (Corin et al., 1983; Lappin et al., 1979; van de Kamp et al., 1990). This protonation/deprotonation equilibrium brings about a local conformational change of residues 35–37. In particular, the peptide unit between residues Pro^{36} and Gly^{37} flips over. The peptide flip induces a movement of two adjacent loops, i.e., the loops that contain residues 9–12 and residues 88–91, respectively, as was confirmed by ^{15}N NMR relaxation experiments performed on wt, Phe^{110}Ser, and Ile^{7}Ser azurin at pH 5.5 (Kalverda, 1996; Kroes, 1997; Kroes et al., manuscript submitted for publication). In the latter studies it was found that amino acids close to His^{35} show higher mobility than more remotely located residues. Hansen et al. (1996) also show that the relative fractions of the two major components are pH dependent, indicating a pH-induced transition from one conformational state to the other. Further studies are planned to investigate the effect of pH on the fluorescence lifetime distributions.

Finally, the effect of a higher viscosity on the fluorescence decays of apo- and holo-azurin has been measured (compare Fig. 3 *C* with Fig. 3 *D*). In the case of the apo-azurins and wt holo-azurin we do not see a significant effect, but the presence of glycerol in the Phe^{110}Ser and Ile^{7}Ser holo-azurin samples produces a significant sharpening of the two main peaks (Fig. 3 *D*). The lifetime distributions in these cases look very similar to the ones displayed in Fig. 3 *A*. The decrease in the widths of the distributions can be interpreted as increased flexibility of the Trp on the time scale of the fluorescence decay and averaging out of the microheterogeneity or as increased rigidity and fixation of the protein framework around one or two well-defined conformations (Bastiaens et al., 1992). The mutants have a cavity close to Trp^{48} as a result of the substitutions of Ile^{7} and Phe^{110} by a serine. The x-ray

TABLE 2 Anisotropy decay parameters determined with global analysis

Protein	λ_{det} (nm)	$\beta 1$	ϕ_{int} (ns)	$\beta 2$	ϕ_{prot} (ns)	$r(0)$	S^2
Oxidized, pH 7.5							
wt	321	—	—	0.17	6.2 (5.0–7.7)	0.17	1
	349	0.08	0.7 (0.3–1.1)	0.06	7.0 (4.0–15)	0.14	0.42
I7S	321	—	—	0.26	5.8 (5.2–6.4)	0.26	1
	349	0.18	0.4 (0.3–0.5)	0.10	7.8 (6.0–11)	0.28	0.36
F110S	321	—	—	0.29	4.7 (4.3–5.3)	0.29	1
	349	0.19	0.4 (0.3–0.5)	0.12	7.7 (6.0–9.2)	0.31	0.38
Oxidized, pH 5.5							
wt	321	—	—	0.16	3.6 (3.0–4.4)	0.16	1
	349	0.09	0.5 (0.3–0.9)	0.06	6.5 (3.5–15)	0.15	0.39
I7S	321	0.09	0.8 (0.4–2.1)	0.18	7.3 (5.0–20)	0.27	0.66
	349	0.18	0.4 (0.3–0.5)	0.10	8.0 (7.5–8.3)	0.28	0.35
F110S	321	0.09	0.6 (0.3–1.4)	0.20	7.8 (6.2–11)	0.29	0.70
	349	0.13	0.3 (0.2–0.6)	0.16	8.0 (6.5–10)	0.29	0.56
Reduced, pH 5.5							
wt	349	0.11	0.1 (0.1–0.8)	0.09	6.5 (5.2–8.4)	0.20	0.44
I7S	349	0.13	0.3 (0.2–0.6)	0.15	2.6 (1.8–4.9)	0.28	0.54
F110S	349	0.10	0.3 (0.1–0.6)	0.15	3.0 (2.3–4.5)	0.25	0.60
Apo, pH 7.5							
wt	321	—	—	0.12	6.5 (5.8–7.2)	0.12	1
	349	0.05	0.3 (0.1–0.9)	0.08	6.7 (5.5–8.6)	0.13	0.63
I7S	321	—	—	0.25	7.0 (6.7–7.4)	0.25	1
	349	0.06	0.2 (0.1–0.6)	0.18	7.6 (7.0–8.4)	0.24	0.74
F110S	321	—	—	0.25	6.8 (6.5–7.2)	0.25	1
	349	0.06	0.4 (0.2–0.8)	0.17	7.8 (7.1–8.8)	0.23	0.76
Apo, pH 5.5							
wt	321	0.03	1.6 (0.1–6.0)	0.10	7.5 (5.9–20)	0.13	0.78
	349	0.02	0.6 (0.0–3.5)	0.09	5.9 (4.9–14)	0.11	0.79
I7S	321	0.03	1.1 (0.1–5.9)	0.22	7.0 (6.3–20)	0.25	0.89
	349	—	—	0.20	8.3 (6.7–11)	0.20	1
F110S	321	0.03	1.5 (0.2–10)	0.23	7.2 (6.4–20)	0.26	0.88
	349	0.05	0.2 (0.0–2.5)	0.11	4.4 (3.5–10)	0.16	0.70

Proteins are at pH 5.5 or 7.5, $T = 20°C$, $\lambda_{exc} = 300$ nm. The 66% confidence limits are given in parentheses. χ^2 varies between 1.1 and 2.0.

structures show that in Phe^{110}Ser azurin this cavity is filled with one to three water molecules (Hammann et al., 1996). It is conceivable that inclusion of glycerol in these cavities may enhance the local rigidity of the protein framework in the neighborhood of Trp^{48}.

The lifetime distribution pattern of reduced wt azurin (measured at $\lambda_{det} = 349$ nm and pH 5.5; see Fig. 4 and Table 1) exhibits five peaks in total, similar to those of oxidized protein (see Fig. 4). In the reduced protein the shorter component is broader and more intense than in the oxidized form, and the longer components are more pronounced in the lifetime distribution pattern of the reduced species than in that of the oxidized species. For both mutants the lifetime distribution of the reduced protein shows differences from the oxidized protein. The peaks of the reduced sample are sharper, and the two main peaks have slightly different positions. Still, the lifetimes of reduced and oxidized azurin are similar, leaving open the possibility that quenching may be caused by energy transfer from Trp^{48} to the Cu site. Alternatively, quenching could be caused by electron transfer from Trp^{48} to a closely situated residue; a possible candidate is Tyr^{108}, which lies at approximately the same distance from Trp^{48} as Cu (~10 Å).

Fluorescence anisotropy decay

The fluorescence anisotropy decay can be analyzed in terms of two rotational correlation times ($\lambda_{det} = 349$ nm; Table 2). The longer one is connected with the tumbling of the whole molecule (ϕ_{prot}), and the shorter one is connected with internal motion (ϕ_{int}). The value of ϕ_{int} is diagnostic of the local movement of Trp^{48} and of the fluxionality of the protein matrix around it. The confidence limits for ϕ_{prot} are broad in most cases (Table 2), encompassing a range of 2–15 ns, whereas the center values fall in the range of 3–8 ns. The findings are in agreement with the results of ^{1}H-^{15}N NMR experiments on wt, Ile^{7}Ser, and Phe^{110}Ser azurin, from which overall tumbling correlation times between 4.8 and 5.8 ns were found (Kalverda, 1996; Kroes, 1997; Kroes et al., manuscript submitted for publication).

Besides the overall tumbling correlation time, other parameters extracted from the experiment are the correlation

time for internal motion, ϕ_{int}, the initial anisotropy, $r(0)$, and the order parameter, S^2, which can be defined independently of a particular model (Eqs. 5–7). A value of $S^2 < 1$ indicates the presence of mobility of the fluorescing moiety. The angle θ and the diffusion coefficient for the restricted internal motion, $D_\perp$, are defined within the framework of a general rotational diffusion model. From Eqs. 6 and 7 it can be seen that θ and $D_\perp$ (at constant ϕ_{int}) follow the trend of S^2: an S^2 less than 1, indicating increased mobility, corresponds to a larger θ and $D_\perp$. If S^2 equals 1, Trp^{48} is fixed with respect to the protein framework, and the angle of displacement is 0.

At pH 7.5, we find that $S^2 = 1$ when $\lambda_{det} = 321$ nm, whereas $S^2 < 1$ when $\lambda_{det} = 349$ nm. This means that with red-edge detection we select a subensemble of protein molecules that exhibit more mobility of Trp^{48}. Petrich and co-workers (1987) also used different detection wavelengths and observed one or more components for the fluorescence anisotropy decay of apo-azurin, in line with our finding that the detection wavelength is an important factor in determining the outcome of the experiment. At pH 5.5 and $\lambda_{det} = 321$ nm, S^2 is < 1 for the mutants, whereas $S^2 = 1$ for wt, indicative of greater mobility of Trp^{48} in the mutants. As discussed in the analysis of the total fluorescence decay, His^{35} may play a role in this pH effect. Comparing apo- and holo-azurin at $\lambda_{det} = 349$ nm shows that apo-protein has larger order parameters; thus Trp^{48} is less mobile in apo-azurin.

The fact that we observe a slightly increased mobility of Trp^{48} in the mutants is in contrast to, but not necessarily in conflict with, the results from x-ray studies on holo-Phe^{110}Ser and Ile^7Ser azurin (Hammann et al., 1996). From the x-ray structures it can be seen (as witnessed by the temperature B-factors) that the dynamics of Trp^{48} are not changed, but that the microenvironment of Trp^{48} has an increased effective dielectric constant, and that the mutated residues have a higher flexibility. In the present experiments the Trp^{48} mobility is observed under red-edge excitation combined with red-shifted detection. It is conceivable that in these experiments a subensemble of molecules is selected that differs from the conformation that is observed in the crystal. Crystal packing forces may have a subtle but decisive influence on the conformation that is stabilized in the crystal.

$r(0)$ is the intrinsic or fundamental anisotropy of Trp and is a function only of the relative orientations of the absorption and emission dipole moments (Ruggiero et al., 1990). For parallel absorption and emission transition dipoles the initial anisotropy is 0.4. Experimental values of $r(0)$ less than 0.4 generally indicate the existence of relaxation processes occurring on a time scale shorter than the lifetime of the excited state or the time resolution of the experiment. In practice the initial anisotropy of Trp in proteins never reaches a value of 0.4 but usually amounts to less than 0.3 (Petrich et al., 1987), similar to what we find in the present study.

In our case red-edge excitation gives a high initial anisotropy ($r(0)$), as it selects the relaxed species, i.e., those in which the orientation of surrounding dipoles corresponds to the relaxed state (Demchenko, 1992). The initial anisotropy is larger in the Phe^{110}Ser and Ile^7Ser azurin mutants (0.28 for the Cu(II)-proteins; Table 2) than in wt. This can be explained if we take into account that the two lowest singlet excited states of indole derivatives, denoted as ^1L_a and ^1L_b, are close in energy and that their relative energies are determined by the environment (Lami and Glasser, 1986; Hansen et al., 1990). Lami and Glasser (1986) suggested that the fluorescence from Trp^{48} in azurin originates from the ^1L_b state. The transition dipole moment for ^1L_b makes an angle of $\sim 70°$ with the long axis of the indole ring and an angle of $\sim 90°$ with the transition moment for ^1L_a. The ^1L_b transition is thought to be solvent insensitive, whereas the energy of the ^1L_a transition shows significant sensitivity to the solvent environment (Meech et al., 1983; Sweeney et al., 1991). A rapid change in the relative order of these ^1L_a and ^1L_b states would reduce the initial anisotropy (Ruggiero et al., 1990). The lower initial anisotropy observed for wt azurin when compared to the Ile^7Ser and Phe^{110}Ser variants may indicate that the protein environment around Trp^{48} is more relaxed in the two mutants.

CONCLUSIONS

The three lifetimes and amplitudes in the total fluorescence decay of the apo-azurins do not depend strongly on detection wavelength, temperature, pH, or viscosity. There are no significant differences observed between wt and Phe^{110}Ser and Ile^7Ser azurin. Contrary to this, in the case of the oxidized holo-azurins the distribution of the two short lifetimes when $\lambda_{det} = 349$ nm changes as any one of these parameters is changed. This points to flexibility of the Trp^{48} on the time scale of the fluorescence decay. In the mutants the distribution around each lifetime becomes narrower in the presence of glycerol, indicating that in the mutants Trp^{48} is more accessible to glycerol, as glycerol reduces structural fluctuations.

The fluorescence anisotropy decay behavior of the Phe^{110}Ser and Ile^7Ser azurin mutants is indicative of slightly more flexibility of the protein matrix and more mobility of the Trp^{48} than in wt azurin. A higher flexibility of the environment of Trp^{48} has also been inferred by Gilardi et al. (1994) from the red shift of the steady-state fluorescence spectrum.

SJK thanks Dr. G. P. van Wezel for critically reading the manuscript.

This work was supported by the Foundation for Chemical Research (SON) under the auspices of the Netherlands Science Organisation (NWO) and by the European Commission under contract ERB/SC1*CT0-00434.

REFERENCES

Adman, E. T. 1991. Copper protein structures. *Adv. Protein Chem.* 42: 144–197.

Adman, E. T., and L. H. Jensen. 1981. Structural features of azurin at 2.7 Å resolution. *Isr. J. Chem.* 21:8–12.

Bastiaens, P. I. H., A. van Hoek, J. A. E. Benen, J. C. Brochon, and A. J. W. G. Visser. 1992. Conformational dynamics and intersubunit energy transfer in wild-type and mutant lipoamide dehydrogenase from *Azotobacter vinelandii. Biophys. J.* 63:839–853.

Beechem, J. M., E. Gratton, M. Ameloot, J. R. Knutson, and L. Brand. 1992. *In* Topics in Fluorescence Spectroscopy, Vol. 2. J. R. Lakowicz, editor. Plenum Press, New York. 241.

Brochon, J. C. 1994. Maximum entropy method of data analysis in time-resolved spectroscopy. *Methods Enzymol.* 240:262–311.

Burstein, E. A., N. S. Vedenkina, and M. N. Ivkova. 1973. Fluorescence and the location of tryptophan residues in protein molecules. *Photochem. Photobiol.* 18:263–279.

Canters, G. W., and G. Gilardi. 1993. Engineering type 1 copper sites in proteins. *FEBS Lett.* 325:39–48.

Corin, A. F., R. Bersohn, and P. E. Cole. 1983. pH dependence of the reduction-oxidation reaction of azurin with cytochrome *c*-551: role of histidine-35 of azurin in electron transfer. *Biochemistry.* 22:2032–2038.

Demchenko, A. P. 1992. Fluorescence and dynamics in proteins. *In* Topics in Fluorescence Spectroscopy, Vol. 3. J. R. Lakowicz, editor. Plenum Press, New York. 65–111.

Dorovska-Taran, V. N., C. Veeger, and A. J. W. G. Visser. 1993. Comparison of the dynamic structure of α-chymotrypsin in aqueous solution and in reversed micelles by fluorescent active-site probing. *Eur. J. Biochem.* 211:47–55.

Farver, O., L. K. Skov, G. Gilardi, G. Pouderoyen, G. W. Canters, S. Wherland, and I. Pecht. 1996. Structure-function correlation of intramolecular electron transfer in wild type and singlet-site mutated azurins. *Chem. Phys.* 204:271–277.

Finazzi-Agrò, A., G. Rotilio, L. Avigliano, P. Guerrieri, V. Boffi, and B. Mondovì. 1970. Environment of copper in *Pseudomonas aeruginosa* azurin: fluorometric approach. *Biochemistry.* 9:2009–2014.

Gilardi, G., G. Mei, N. Rosato, G. W. Canters, and A. Finazzi-Agrò. 1994. Unique environment of Trp^{48} in *Pseudomonas aeruginosa* azurin as probed by site-directed mutagenesis and dynamic fluorescence spectroscopy. *Biochemistry.* 33:1425–1432.

Grinvald, A., J. Schlessinger, I. Pecht, and I. Z. Steinberg. 1975. Homogeneity and variability in the structure of azurin molecules studied by fluorescence decay and circular polarization. *Biochemistry.* 14: 1921–1929.

Hammann, C., A. Messerschmidt, R. Huber, H. Nar, G. Gilardi, and G. W. Canters. 1996. X-ray crystal structure of the two site-specific mutants $Ile^{7}Ser$ and $Phe^{110}Ser$ of azurin from *Pseudomonas aeruginosa. J. Mol. Biol.* 255:362–366.

Hansen, J. E., J. W. Longworth, and G. R. Fleming. 1990. Photophysics of metalloazurins. *Biochemistry.* 29:7329–7338.

Hansen, J. E., D. G. Steel, and A. Gafni. 1996. Detection of a pH-dependent conformational change in azurin by time-resolved phosphorescence. *Biophys. J.* 71:2138–2143.

Hutnik, C. M., and A. G. Szabo. 1989a. Confirmation that multiexponential fluorescence decay behavior of holo-azurin originates from conformational heterogeneity. *Biochemistry.* 28:3923–3934.

Hutnik, C. M., and A. G. Szabo. 1989b. A time-resolved fluorescence study of azurin and metalloazurin derivatives. *Biochemistry.* 28: 3935–3939.

Kalverda, A. P. 1996. Backbone dynamics of azurin as studied by N-15 relaxation times. Ph.D. thesis. University of Leiden, Leiden, The Netherlands.

Kim, S. J., F. N. Chowdhury, W. Stryjewski, E. S. Younathan, P. S. Russo, and M. D. Barkley. 1993. Time-resolved fluorescence of the single tryptophan of *Bacillus stearothermophilus* phosphofructokinase. *Biophys. J.* 65:215–226.

Kinosita, K., S. Kawata, and A. Ikegami. 1977. A theory of fluorescence polarization decay in membranes. *Biophys. J.* 20:289–305.

Kraulis, P. J. 1991. MOLSCRIPT: a program to produce both detailed and schematic plots of protein structures. *J. Appl. Crystallogr.* 24:946–950.

Kroes, S. J. 1997. Structural analysis of mutants of the blue copper protein azurin. Ph.D. thesis. University of Leiden, Leiden, The Netherlands. 151 pp.

Lakowicz, J. R. 1983. Principles of Fluorescence Spectroscopy. Plenum Press, New York.

Lakowicz, J. R., and S. Keating-Nakamoto. 1984. Red-edge excitation of fluorescence and dynamic properties of proteins and membranes. *Biochemistry.* 23:3013–3021.

Lami, H., and N. Glasser. 1986. Indole's solvatochromism revisited. *J. Chem. Phys.* 84:597–604.

Lappin, A. G., M. G. Segal, D. C. Weatherburn, R. A. Henderson, and A. G. Sykes. 1979. Kinetic studies on 1:1 electron-transfer reactions involving blue copper proteins. 3. Protonation effects, protein-complex association, and binding sites in reactions of *Pseudomonas aeruginosa* azurin with $Co(phen)_3^{3+}$, $Co(4,7\text{-}DPSphen)_3^{3-}$, and $Fe(CN)_6^{3-}$ (oxidants) and $Fe(CN)_6^{4-}$ (reductant). *J. Am. Chem. Soc.* 101:2302–2306.

Leenders, R., M. Kooijman, A. van Hoek, C. Veeger, and A. J. W. G. Visser. 1993. Flavin dynamics in reduced flavodoxins. *Eur. J. Biochem.* 211:37–45.

Lipari, G., and A. Szabo. 1982. Model-free approach to the interpretation of nuclear magnetic resonance relaxation in macromolecules. 1. Theory and range of validity. *J. Am. Chem. Soc.* 104:4546–4559.

Livesey, A. K., and J. C. Brochon. 1987. Recovering the distribution of decay constants in pulse-fluorimetry using maximum entropy. *Biophys. J.* 52:693–706.

Meech, S. R., D. Phillips, and A. G. Lee. 1983. On the nature of the fluorescent state of methylated indole derivatives. *Chem. Phys.* 80: 317–328.

Mei, G., G. Gilardi, M. Venanzi, N. Rosato, G. W. Canters, and A. Finazzi-Agrò. 1996. Probing the structure and mobility of *Pseudomonas aeruginosa* azurin by circular dichroism and dynamic fluorescence anistropy. *Protein Sci.* 5:2248–2254.

Munro, I., I. Pecht, and L. Stryer. 1979. Subnanosecond motions of tryptophan residues in proteins. *Proc. Natl. Acad. Sci. USA.* 76:55–60.

Nar, H., A. Messerschmidt, R. Huber, M. van de Kamp, and G. W. Canters. 1991a. X-ray crystal structure of the two site-specific mutants $His^{35}Gln$ and $His^{35}Leu$ of azurin from *Pseudomonas aeruginosa. J. Mol. Biol.* 218:427–447.

Nar, H., A. Messserschmidt, R. Huber, M. van de Kamp, and G. W. Canters. 1991b. Crystal structure analysis of oxidized *Pseudomonas aeruginosa* azurin at pH 5.5 and 9.0. *J. Mol. Biol.* 221:765–772.

Pap, E. H. W., P. I. H. Bastiaens, J. W. Borst, P. A. W. van den Berg, A. van Hoek, G. T. Snoek, K. W. A. Wirtz, and A. J. W. G. Visser. 1993. Quantitation of the interaction of protein kinase C with diacylglycerol and phosphoinositides by time-resolved detection of resonance energy transfer. *Biochemistry.* 32:13310–13317.

Petrich J. W., J. W. Longworth, and G. R. Fleming. 1987. Internal motion and electron transfer in proteins: a picosecond fluorescence study of three homologous azurins. *Biochemistry.* 26:2711–2722.

Ruggiero, A. J., D. C. Todd, and G. R. Fleming. 1990. Subpicosecond fluorescence anisotropy studies of tryptophan in water. *J. Am. Chem. Soc.* 112:1003–1014.

Solomon, E. I., M. J. Baldwin, and M. Lowery. 1992. Electronic structures of active sites in copper proteins: contributions to reactivity. *Chem. Rev.* 92:521–542.

Sweeney, J. A., P. A. Harmon, S. A. Asher, C. M. Hutnik, and A. G. Szabo. 1991. UV resonance Raman examination of the azurin tryptophan environment and energy relaxation pathways. *J. Am. Chem. Soc.* 113: 7531–7537.

Szabo, A. 1984. Theory of fluorescence depolarization in macromolecules and membranes. *J. Chem. Phys.* 81:150–167.

Szabo, A. G., T. M. Stepanik, D. M. Wayner, and N. M. Young. 1983. Conformational heterogeneity of the copper binding site in azurin—a time-resolved fluorescence study. *Biophys. J.* 41:233–244.

van de Kamp, M., F. C. Hali, N. Rosato, A. Finazzi Agro, and G. W. Canters. 1990. Purification and characterization of a non-reconstitutable azurin, obtained by heterologous expression of *Pseudomonas aeruginosa azu* gene in *Escherichia coli. Biochim. Biophys. Acta.* 1019: 283–292.

Visser, N. V., A. J. W. G. Visser, T. Konc, P. Kroh, and A. van Hoek. 1994. New reference compound with single, ultrashort lifetime for time-resolved tryptophan fluorescence experiments. *Proc. SPIE.* 2137: 618–626.